PERGAMON

PII: S1359-6454(98)00381-4

Acta mater. Vol. 47, No. 2, pp. 385–395, 1999

Printed in Great Britain
1359-6454/99 $19.00 + 0.00

TRACER DIFFUSION OF Au AND Cu IN A SERIES OF NEAR $\Sigma = 5$ (310)[001] SYMMETRICAL Cu TILT GRAIN BOUNDARIES

E. BUDKE[1], T. SURHOLT[1], S. I. PROKOFJEV[2], L. S. SHVINDLERMAN[2] and CHR. HERZIG[1]†

[1]Institut für Metallforschung, Universität Münster, Wilhelm-Klemm-Str. 10, D-48149 Münster, Germany and [2]Institute of Solid State Physics, Russian Academy of Sciences, 142432 Chernogolovka, Moscow Distr., Russia

(Received 15 June 1998; accepted 29 October 1998)

Abstract—Grain boundary diffusion of Au and Cu was measured in a series of Cu bicrystals with symmetrical near $\Sigma = 5$, $\Theta = 36.9°$ (310)[001] CSL tilt grain boundaries (GBs) using the radiotracer and the serial sectioning technique. The orientations of the bicrystals were very precisely determined with the Kossel technique where all three macroscopic parameters describing the orientations of the grains in the bicrystal were evaluated. The tilt angles ranged from 33.21° to 39.26°. The GB diffusion of the radiotracers ^{195}Au and ^{64}Cu was measured as a function of tilt angle and temperature. In the investigated temperature range 1030–661 K the orientation dependence of both radiotracers shows a characteristic cusp not exactly at but slightly below the ideal $\Sigma = 5$ CSL GB. The Arrhenius parameters, activation enthalpy and frequency factor, determined from lower temperature data adopt a maximum, again slightly before the ideal $\Sigma = 5$ CSL GB. These features are discussed with respect to the accidental small twist and second tilt orientations and the corresponding dislocation network inherent in the investigated real GBs. With increasing temperature a negative deviation from a straight Arrhenius behaviour is observed. This result indicates a certain change in the GB structure in the temperature range above 800 K. © *1999 Acta Metallurgica Inc. Published by Elsevier Science Ltd. All rights reserved.*

1. INTRODUCTION

A number of investigations were carried out in the last few decades to relate the behaviour of grain boundary (GB) diffusion to the structure of GBs. The results of these works and the given interpretations are to some extent contradictory.

On the one hand sharp narrow cusps of GB diffusivity and peaks of Arrhenius parameters are reported at certain GBs of high coincidence [1–5]. Grain boundaries of high coincidence and therefore of highly ordered atomic structure are expected to yield minima in diffusivity and maxima in Arrhenius parameters due to the larger mean vacancy formation and migration enthalpies in comparison to GBs of low coincidence and of lower degree of perfection [6]. Unfortunately, the experiments supporting the CSL model were performed using solute GB diffusion in combination with electron microprobe analysis. Due to the rather large required solute concentrations in the GBs in such an analysis, these studies were carried out, in fact, under conditions of chemical diffusion. This sets serious obstacles to the interpretation of the deduced GB diffusion parameters and the observed minima and maxima in $s\delta D_{GB}$. It was argued [7] that the observed minima might be related to the structural dependence of solute GB segregation which is included in the GB diffusion parameters in type-B kinetics of solute diffusion.

On the other hand a possible continuous relationship between GB diffusion and the macroscopic grain orientation of symmetrical [001] tilt GBs is supposed. Sommer *et al.* [8] investigated self-diffusion along bonded symmetrical [001] Ag tilt GBs and found a continuous variation of δD_{GB} with the tilt angle Θ. The tilt angle Θ describes the grain orientation of the two adjacent grains with respect to the [001] tilt axis. Ma and Balluffi [9] studied Ag diffusion in a series of [001] Au tilt GBs in thin films at low temperatures using a surface accumulation technique in combination with Auger spectroscopy. Again, a continuous variation of δD_{GB} was observed. These results were interpreted in terms of the structural unit model for diffusion [10, 11]. This model considers the core of symmetrical [001] tilt GBs as binary arrangements of structural units. These structural units are derived from two nearby delimiting boundaries which are made up of one unique type of structural unit. Variations in the tilt angle Θ lead to a continuous change in the fractional arrangement of both types of structural units of the delimiting boundaries. Therefore, GB diffusion is supposed to change con-

†To whom all correspondence should be addressed.

tinuously with the variation of Θ. It should be pointed out that the distance in the tilt angle Θ between the experimental points in the investigations of Sommer *et al.* [8] as well as of Ma and Balluffi [9] were comparably large (5–10°). These studies therefore yield no proof in favour of the structural unit model of GB diffusion, if possible cusps turn out to be rather narrow.

The aim of the present study is to overcome the previous obstacles for a clear decision between the two conflicting considerations about the relation of diffusion in oriented GBs and their individual atomistic structure. Therefore, using the radiotracer ^{195}Au, the diffusion of Au was studied in the present paper along a series of symmetrical [001] tilt GBs of Cu with tilt angles Θ in the range 33.21–39.26° in the vicinity of the ideal $\Sigma = 5$, $\Theta = 36.9°$ (310)[001] tilt boundary. The precise radiotracer technique in combination with the serial sectioning method of the diffusion zone enables us to obtain accurate GB diffusion profiles in a single GB. The application of carrier free ^{195}Au radiotracer with very high specific activity and a high-efficiency detector system allows very small concentrations of the diffusant in the GBs. Thus any disturbance of the GB structure is almost excluded. Furthermore, the Au–Cu phase diagram [12] suggests weak chemical interactions between Au and Cu atoms. Effects of Au segregation therefore are expected to be rather small. Nevertheless, in order to check the reliability of our measured orientation dependence of Au GB diffusion in Cu, the GB self-diffusion was also studied at one temperature with the ^{64}Cu radiotracer of short half-life, which impedes a full systematic study with this Cu radiotracer.

2. EXPERIMENTAL

The Cu bicrystals were grown in a graphite mould in high purity argon atmosphere by directional crystallization using Cu single crystals of high purity (nominal 99.995%) Cu. It should be pointed out that the purity of the bicrystals used for the diffusion measurements was higher than the nominal purity of the initial Cu material since the technique of growing bicrystals acts like a zone refinement of the Cu material. Bicrystals of 16×3 mm^2 in cross-section and with lengths up to 200 mm were grown.

The orientations of the grains of each bicrystal were determined by Kossel-technique measurements. The advantage of this technique is that it can measure all three macroscopic parameters describing the orientation of the adjacent grains with very high precision. Table 1 contains the resulting tilt angles Θ with respect to the [001] axis, the twist angles Φ with respect to the [310] axis and the second tilt angles Ψ with respect to the [$\bar{1}$30] axis. The orientation of the GB plane was carefully adjusted during the bicrystal growth process but was not explicitly remeasured.

Quadratic diffusion samples (6×6 mm^2) were cut from the bicrystals by spark erosion and cleaned by chemical etching in nitric acid. One front (001) surface of each specimen was mechanically polished by standard metallographic procedures and finished by electrolytical polishing. The electrolytical polishing procedure removes the dislocation enriched surface layer resulting from the mechanical polishing process.

The samples were sealed in quartz ampoules under purified argon atmosphere ($\approx 10^2$ Pa) and were annealed first at 1173 K for two days and furthermore under the conditions (temperature T, time t—at least, however, for two weeks) of the intended diffusion anneals in order to achieve quasi-equilibrium GB segregation of spurious impurities and to prove the stability of the GB. The GB quality was checked by optical microscopy. Slightly curved GBs indicate changing inclinations along the GB leading to different crystallographic orientations of the GBs which is accompanied by a change in the GB structure. Such specimens were discarded.

The carrier-free radiotracer ^{195}Au (half-life 183 days) was used in this work in the form of a HCl solution with an initial specific activity of about 63×10^6 Bq/μg. For the GB self-diffusion measurements, the radiotracer ^{64}Cu (half-life 12.7 h) was produced from the nuclear reaction ^{63}Cu$(n,\gamma)^{64}$Cu with initial specific activity of 0.26×10^6 Bq/μg by means of exposing copper with natural isotope composition to neutron radiation at a reactor (GKSS Forschungszentrum, Geesthacht, Germany). Immediately after radiation the radioactive Cu was delivered within a few hours to our laboratory in Münster and was dissolved in diluted nitric acid. Both ^{195}Au and ^{64}Cu radiotracers were dropped onto the polished surface of the Cu speci-

Table 1. Orientations of the investigated Cu bicrystals with orientations near the $\Sigma = 5$, $\Theta = 36.9°$ (310)[001] CSL GB, determined by Kossel-technique measurements. Θ: tilt angle with respect to the [001] axis, Φ: twist angle with respect to the [310] axis, Ψ: tilt angle with respect to the [$\bar{1}$30] axis

No.	Θ (°)	Φ (°)	Ψ (°)
1	33.21 ± 0.18	0.80 ± 0.15	0.47 ± 0.15
2	33.60 ± 0.08	0.60 ± 0.15	0.20 ± 0.13
3	35.10 ± 0.04	0.05 ± 0.01	0.75 ± 0.02
4	35.19 ± 0.03	0.22 ± 0.04	1.72 ± 0.03
5	35.88 ± 0.20	0.95 ± 0.10	2.03 ± 0.16
6	36.00 ± 0.29	0.25 ± 0.10	2.50 ± 0.02
7	36.26 ± 0.37	0.05 ± 0.10	1.15 ± 0.17
8	36.26 ± 0.37	0.55 ± 0.25	0.90 ± 0.19
9	36.53 ± 0.09	0.10 ± 0.15	1.10 ± 0.12
10	36.67 ± 0.17	1.85 ± 0.20	1.12 ± 0.23
11	36.97 ± 0.02	1.27 ± 0.06	0.42 ± 0.02
12	37.20 ± 0.29	0.60 ± 0.20	0.11 ± 0.15
13	37.45 ± 0.03	1.27 ± 0.01	1.14 ± 0.03
14	37.57 ± 0.10	1.30 ± 0.10	0.11 ± 0.02
15	37.74 ± 0.08	1.80 ± 0.05	0.15 ± 0.03
16	38.12 ± 0.30	0.30 ± 0.35	0.76 ± 0.16
17	39.26 ± 0.26	0.50 ± 0.45	0.30 ± 0.13

mens and dried. The initial surface activity of each sample ranged from 2×10^4 to 3×10^4 Bq for the Au radiotracer and from 10^5 to 10^6 Bq for the Cu radiotracer, depending in the latter case on the chosen diffusion annealing time of the sample.

Usually several bicrystals were annealed in the same ampoule under purified argon atmosphere for the actual diffusion annealings. The Au diffusion measurements were performed at six temperatures in the temperature range 1030–661 K and the self-diffusion measurements at the temperature 919 K. The temperatures were measured with Ni/NiCr thermocouples and controlled within ± 1 K. After the diffusion annealings the specimens were reduced in diameter to eliminate the effect of radial diffusion and were sectioned on a microtome. The thickness of each section was determined from its weight, diameter and the density of Cu. The intensity of the decays of ^{195}Au and ^{64}Cu in each section was detected with a liquid scintillation counter of very low background and automatic sample changer.

3. RESULTS

The diffusion time t for all studied temperatures was chosen so that all measurements were carried out in the type-B kinetic regime [13, 14]. Typical penetration profiles of ^{195}Au are shown in Figs 1(a) and (b) and ^{64}Cu GB diffusion profiles in Cu bicrystals are shown in Fig. 2. The profiles were plotted as $\ln \bar{c}$ vs $y^{6/5}$. The GB diffusion related tails were fitted by straight lines. From the slopes $\partial \ln \bar{c}/\partial y^{6/5}$ the values of GB diffusivity $s\delta D_{GB}$ (s: solute GB segregation factor; $s = 1$ for GB self-diffusion, δ: GB width, D_{GB}: GB diffusion coefficient) were calculated using the Suzuoka solution of the GB diffusion equation, which implies instantaneous source conditions

$$s\delta D_{GB} = 2q^p D^r t^{-u} \left(-\frac{\partial \ln \bar{c}}{\partial y^{6/5}} \right)^{-p} \qquad (1)$$

where $p = 1.6807$, $q = 0.740$, $r = 0.4916$ and $u = 0.5084$ in typical experimental conditions when the parameter $10^2 < \beta = (s\delta D_{GB})/(2D^{3/2}t^{1/2}) < 10^4$ [13, 14]. These parameters change slightly for other ranges of β [13]. According to the B regime, the conditions $\beta > 10$ and $\alpha = s\delta/2(Dt)^{1/2} \ll 1$ are fulfilled, see Tables 2–7.

The lattice diffusion coefficient D of Au in Cu follows the Arrhenius relations

$$D^{Au}(T) = 8.0 \times 10^{-6} \cdot \exp\left(-\frac{191.1 \text{ kJ/mol}}{RT} \right) \text{ m}^2/\text{s} \qquad (2)$$

in the temperature range $982 \text{ K} \geq T \geq 633$ K and

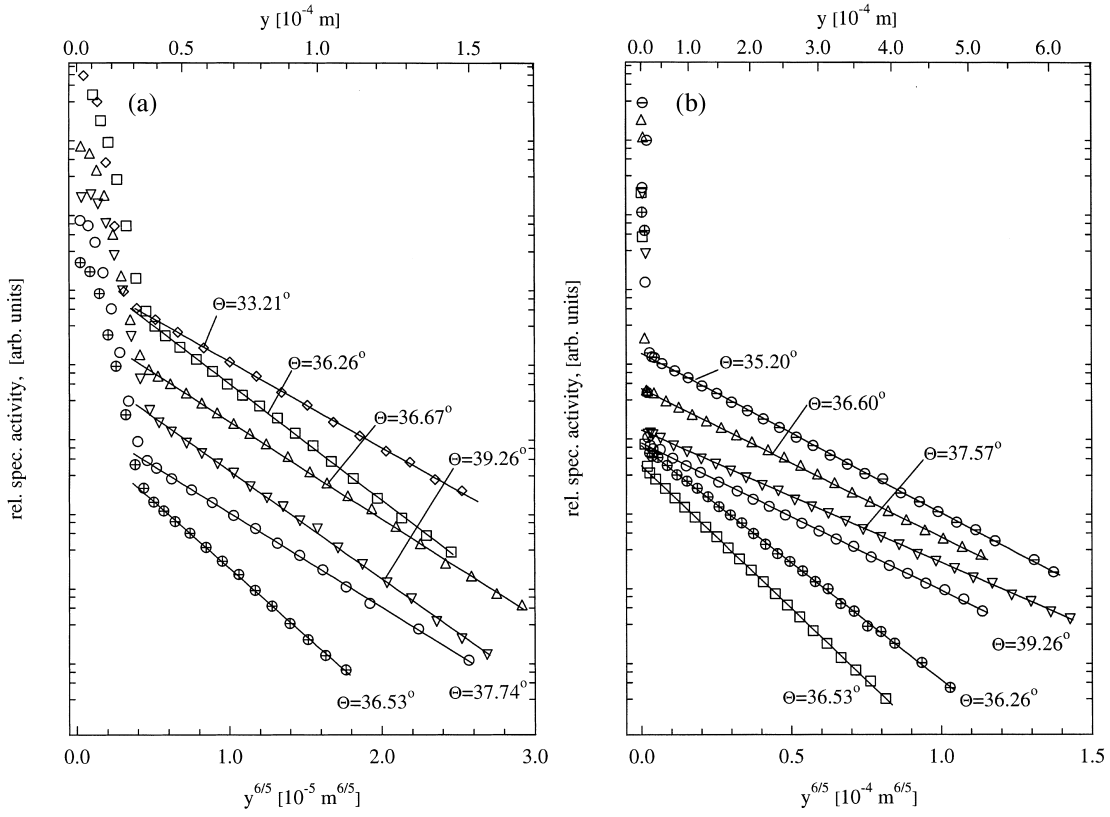

Fig. 1. Tracer penetration profiles of ^{195}Au in symmetrical near $\Sigma = 5$, $\Theta = 36.9°$ (310)[001] Cu tilt GBs after diffusion annealing at $T = 1030$ K for $t = 15\,120$ s (a) and at $T = 780$ K for $t = 247\,620$ s (b).

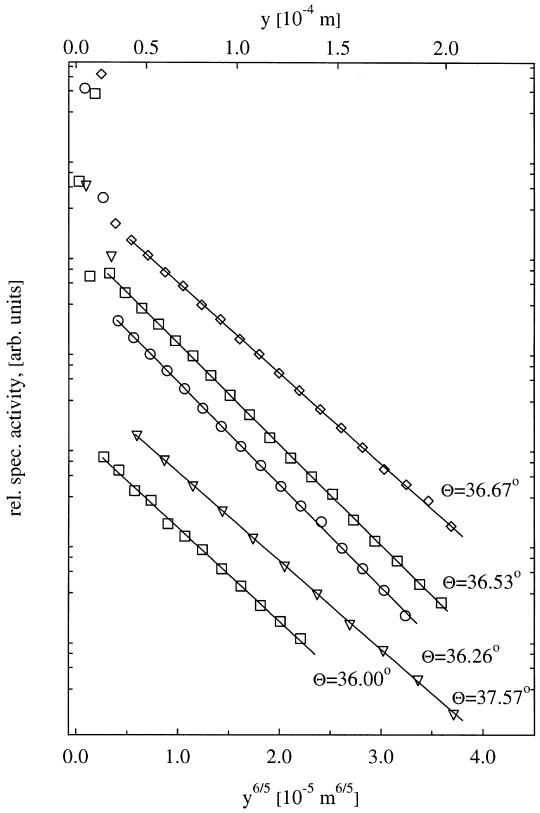

Fig. 2. Tracer penetration profiles of ^{64}Cu in symmetrical near $\Sigma = 5$, $\Theta = 36.9^\circ$ (310)[001] Cu tilt GBs after diffusion annealing at $T = 919$ K for $t = 34\,560$ s.

$$D^{\mathrm{Au}}(T) = 5.4 \times 10^{-5} \cdot \exp\left(-\frac{205.6\ \mathrm{kJ/mol}}{RT}\right)\ \mathrm{m^2/s} \quad (3)$$

in the high temperature range $1350\ \mathrm{K} \geq T \geq 993$ K [15]. The Arrhenius relation

$$D^{\mathrm{Cu}}(T) = 1.0 \times 10^{-5} \cdot \exp\left(-\frac{196.8\ \mathrm{kJ/mol}}{RT}\right)\ \mathrm{m^2/s} \quad (4)$$

Table 2. Results and experimental parameters of ^{195}Au diffusion along [001] tilt GBs with different tilt angles Θ in symmetrical near $\Sigma = 5$, $\Theta = 36.9^\circ$ (310)[001] GBs. $T = 1030$ K, $t = 15\,120$ s, $D = 2.01 \times 10^{-15}$ m^2/s, $\alpha = s{\cdot}4.53 \times 10^{-5}$

No.	Θ (°)	$s\delta D_{\mathrm{GB}}$ (m^2/s)	β
1	33.21 ± 0.18	$2.45 \times 10^{-19} \pm 1.93\%$	11
3	35.10 ± 0.04	$2.37 \times 10^{-19} \pm 1.42\%$	11
4	35.19 ± 0.03	$2.52 \times 10^{-19} \pm 1.39\%$	11
5	35.88 ± 0.20	$2.18 \times 10^{-19} \pm 2.17\%$	9.8
6	36.00 ± 0.29	$2.65 \times 10^{-19} \pm 1.41\%$	12
6	36.00 ± 0.29	$2.65 \times 10^{-19} \pm 1.78\%$	12
7	36.26 ± 0.37	$2.40 \times 10^{-19} \pm 0.96\%$	11
9	36.53 ± 0.09	$1.86 \times 10^{-19} \pm 1.03\%$	8.4
10	36.67 ± 0.17	$3.24 \times 10^{-19} \pm 0.85\%$	14.6
14	37.57 ± 0.10	$3.62 \times 10^{-19} \pm 1.85\%$	16
15	37.74 ± 0.08	$3.42 \times 10^{-19} \pm 1.05\%$	15
16	38.12 ± 0.30	$3.38 \times 10^{-19} \pm 1.19\%$	15
17	39.26 ± 0.26	$2.72 \times 10^{-19} \pm 0.84\%$	12

used for evaluating the GB self-diffusion in Cu has been determined in the temperature range $905\ \mathrm{K} \geq T \geq 574$ K [16]. The resulting GB diffusion parameters $s\delta D_{\mathrm{GB}}$ of ^{195}Au and ^{64}Cu in Cu are listed together with other relevant experimental parameters in Tables 2–7.

The high quality of the measured diffusion profiles in Figs 1(a) and (b) and Fig. 2 shows as in our study on Al bicrystals [17] that the underlying mathematical conditions of the Suzuokas solution can be exactly realized in GB diffusion experiments on bicrystals. The uncertainty in the slope of the GB diffusion profiles is less than 1% in most cases, i.e. the GB diffusion parameter is determined extremely accurately for this set of bicrystals. Such good linearity over several orders of magnitude in concentration is usually not observed in polycrystalline samples due to the presence of differently behaving GBs [18] and due to the occurrence of some slight GB motion [19, 20].

3.1. Orientation dependence of the grain boundary diffusion parameter $s\delta D_{\mathrm{GB}}$

The dependence of the GB diffusion parameter $s\delta D_{\mathrm{GB}}$ on the tilt angle Θ in the temperature range 1030–661 K is shown for ^{195}Au in Figs 3(a) and (b) for four temperatures. At smaller tilt angles $s\delta D_{\mathrm{GB}}(\Theta)$ increases monotonously with increasing tilt angle Θ. At $\Theta = 36.53^\circ$ a characteristic minimum of $s\delta D_{\mathrm{GB}}$ is observed, slightly before the ideal $\Sigma = 5$, $\Theta = 36.9^\circ$ (310)[001] GB. In the immediate vicinity of the ideal $\Sigma = 5$ CSL GB the GB diffusivity seems to increase drastically within only a few tenths of a degree in the tilt angle variation. Behind the ideal $\Sigma = 5$ GB, $s\delta D_{\mathrm{GB}}$ seems to decrease with increasing tilt angle Θ. The variation of $s\delta D_{\mathrm{GB}}(\Theta)$ is not symmetrical to the $\Sigma = 5$ GB. The observed cusp at $\Theta = 36.53^\circ$ becomes more pronounced with decreasing temperature. Qualitatively the same characteristic orientation dependence of $\delta D_{\mathrm{GB}}(\Theta)$ is also observed for the GB self-diffusion at $T = 919$ K, see Fig. 4. Again, $\delta D_{\mathrm{GB}}(\Theta)$ reveals a cusp not exactly at but slightly below the ideal $\Sigma = 5$ CSL GB.

Table 3. Results and experimental parameters of ^{195}Au diffusion along [001] tilt GBs with different tilt angles Θ in symmetrical near $\Sigma = 5$, $\Theta = 36.9^\circ$ (310)[001] GBs. $T = 978$ K, $t = 20\,430$ s, $D = 5.03 \times 10^{-16}$ m^2/s, $\alpha = s{\cdot}7.80 \times 10^{-5}$

No.	Θ (°)	$s\delta D_{\mathrm{GB}}$ (m^3/s)	β
1	33.21 ± 0.18	$1.80 \times 10^{-19} \pm 0.98\%$	2.0×10^4
4	35.19 ± 0.03	$1.65 \times 10^{-19} \pm 1.77\%$	3.1×10^4
5	35.88 ± 0.20	$1.44 \times 10^{-19} \pm 2.37\%$	3.7×10^4
6	36.00 ± 0.29	$2.03 \times 10^{-19} \pm 0.84\%$	2.7×10^4
7	36.26 ± 0.37	$1.88 \times 10^{-19} \pm 1.27\%$	1.6×10^4
9	36.53 ± 0.09	$1.31 \times 10^{-19} \pm 1.40\%$	1.2×10^4
10	36.67 ± 0.17	$2.18 \times 10^{-19} \pm 0.95\%$	3.5×10^4
14	37.57 ± 0.10	$2.23 \times 10^{-19} \pm 1.07\%$	4.2×10^4
15	37.74 ± 0.08	$2.77 \times 10^{-19} \pm 2.32\%$	6.1×10^4
16	38.12 ± 0.30	$2.42 \times 10^{-19} \pm 1.49\%$	4.0×10^4
17	39.26 ± 0.26	$1.87 \times 10^{-19} \pm 1.80\%$	3.6×10^4

Table 4. Results and experimental parameters of ^{195}Au diffusion along [001] tilt GBs with different tilt angles Θ in symmetrical near $\Sigma = 5$, $\Theta = 36.9^\circ$ (310)[001] GBs. $T_1 = 872$ K, $T_2 = 868$ K, $t = 67\,392$ s, $D_1 = 2.89 \times 10^{-17}$ m^2/s, $\alpha_1 = s \cdot 1.79 \times 10^{-4}$, $D_2 = 2.56 \times 10^{-17}$ m^2/s, $\alpha_2 = s \cdot 1.90 \times 10^{-4}$

No.	T (K)	Θ (°)	$s\delta D_{GB}$ (m^3/s)	β
1	T_1	33.21 ± 0.18	$8.61 \times 10^{-20} \pm 1.59\%$	1067
2	T_1	33.60 ± 0.08	$7.28 \times 10^{-20} \pm 1.52\%$	903
3	T_2	35.10 ± 0.04	$7.09 \times 10^{-20} \pm 1.48\%$	1054
4	T_2	35.19 ± 0.03	$8.03 \times 10^{-20} \pm 0.83\%$	1195
5	T_1	35.88 ± 0.20	$1.23 \times 10^{-19} \pm 0.93\%$	1519
6	T_2	36.00 ± 0.29	$8.40 \times 10^{-20} \pm 0.60\%$	1248
6	T_2	36.00 ± 0.29	$8.51 \times 10^{-20} \pm 0.62\%$	1266
7	T_2	36.26 ± 0.37	$8.44 \times 10^{-20} \pm 0.61\%$	1255
8	T_1	36.26 ± 0.37	$1.15 \times 10^{-19} \pm 2.63\%$	1468
9	T_1	36.53 ± 0.09	$7.01 \times 10^{-20} \pm 0.65\%$	461
10	T_1	36.67 ± 0.17	$1.46 \times 10^{-19} \pm 0.73\%$	1809
12	T_2	37.20 ± 0.29	$8.50 \times 10^{-20} \pm 1.33\%$	1264
14	T_2	37.57 ± 0.10	$1.17 \times 10^{-19} \pm 0.77\%$	1732
16	T_1	38.12 ± 0.30	$1.41 \times 10^{-19} \pm 0.45\%$	1747
17	T_2	39.26 ± 0.26	$9.38 \times 10^{-20} \pm 0.78\%$	1395

3.2. Orientation dependence of the grain boundary diffusion Arrhenius parameters

The temperature dependence of ^{195}Au GB diffusion of all bicrystals is shown in Figs 5(a)–(d) in Arrhenius coordinates. In the whole investigated temperature range the measured $s\delta D_{GB}$ values of the bicrystals, with the exception of bicrystal No. 14, do not follow the linear Arrhenius relation

$$s\delta D_{GB}(T) = (s\delta D_{GB})_0 \cdot \exp\left(-\frac{Q_{GB}}{RT}\right) \qquad (5)$$

($(s\delta D_{GB})_0$: pre-exponential factor, Q_{GB}: effective activation enthalpy of GB diffusion). A rather concave curvature is observed at high temperatures. Therefore, the experimentally determined points were fitted by Arrhenius lines only in the lower temperature range, see Figs 5(a)–(d). Due to the high precision of $s\delta D_{GB}$ these fits are regarded as meaningful. The resulting pre-exponential factor $(s\delta D_{GB})_0$ and the effective activation enthalpy Q_{GB} for each orientation Θ are listed together with the corresponding temperature range of these fits in Table 8.

Table 5. Results and experimental parameters of ^{195}Au diffusion along [001] tilt GBs with different tilt angles Θ in symmetrical near $\Sigma = 5$, $\Theta = 36.9^\circ$ (310)[001] GBs. $T = 780$ K, $t = 247\,620$ s, $D = 1.29 \times 10^{-18}$ m^2/s, $\alpha = s \cdot 4.42 \times 10^{-4}$

No.	Θ (°)	$s\delta D_{GB}$ (m^3/s)	β
1	33.21 ± 0.18	$2.96 \times 10^{-20} \pm 0.49\%$	2.0×10^4
3	35.10 ± 0.04	$4.52 \times 10^{-20} \pm 0.80\%$	3.1×10^4
4	35.19 ± 0.03	$4.53 \times 10^{-20} \pm 0.72\%$	3.1×10^4
5	35.88 ± 0.20	$5.44 \times 10^{-20} \pm 0.56\%$	3.7×10^4
6	36.00 ± 0.29	$3.99 \times 10^{-20} \pm 1.28\%$	2.7×10^4
6	36.00 ± 0.29	$3.53 \times 10^{-20} \pm 0.69\%$	2.4×10^4
7	36.26 ± 0.37	$2.39 \times 10^{-20} \pm 0.72\%$	1.6×10^4
7	36.26 ± 0.37	$3.01 \times 10^{-20} \pm 1.57\%$	2.0×10^4
9	36.53 ± 0.09	$1.71 \times 10^{-20} \pm 0.52\%$	1.2×10^4
9	36.53 ± 0.09	$2.21 \times 10^{-20} \pm 1.23\%$	1.5×10^4
10	36.67 ± 0.17	$5.13 \times 10^{-20} \pm 0.68\%$	3.5×10^4
11	36.97 ± 0.02	$6.08 \times 10^{-20} \pm 0.82\%$	4.2×10^4
12	37.20 ± 0.29	$5.34 \times 10^{-20} \pm 0.64\%$	3.7×10^4
12	37.20 ± 0.29	$7.77 \times 10^{-20} \pm 0.61\%$	5.3×10^4
13	37.45 ± 0.03	$7.33 \times 10^{-20} \pm 0.60\%$	5.0×10^4
14	37.57 ± 0.10	$6.19 \times 10^{-20} \pm 0.54\%$	4.2×10^4
15	37.74 ± 0.08	$8.93 \times 10^{-20} \pm 0.65\%$	6.1×10^4
16	38.12 ± 0.30	$5.85 \times 10^{-20} \pm 0.64\%$	4.0×10^4
16	38.12 ± 0.30	$6.51 \times 10^{-20} \pm 0.96\%$	4.5×10^4
17	39.26 ± 0.26	$5.18 \times 10^{-20} \pm 0.71\%$	3.6×10^4

Table 6. Results and experimental parameters of ^{195}Au diffusion along [001] tilt GBs with different tilt angles Θ in symmetrical near $\Sigma = 5$, $\Theta = 36.9^\circ$ (310)[001] GBs. $T = 661$ K, $t_1 = 5\,673\,360$ s, $t_2 = 5\,680\,595$ s, $D = 6.42 \times 10^{-21}$ m^2/s, $\alpha = s \cdot 1.31 \times 10^{-3}$

No.	Θ (°)	$s\delta D_{GB}$ (m^3/s)	t (s)	β
1	33.21 ± 0.18	$3.54 \times 10^{-21} \pm 0.58\%$	t_1	1.4×10^6
3	35.10 ± 0.04	$5.83 \times 10^{-21} \pm 0.84\%$	t_2	2.4×10^6
4	35.19 ± 0.03	$8.52 \times 10^{-21} \pm 0.60\%$	t_2	3.5×10^6
5	35.88 ± 0.20	$7.65 \times 10^{-21} \pm 1.02\%$	t_1	3.1×10^6
6	36.00 ± 0.29	$6.12 \times 10^{-21} \pm 0.50\%$	t_1	2.5×10^6
7	36.26 ± 0.37	$3.02 \times 10^{-21} \pm 0.66\%$	t_1	1.2×10^6
7	36.26 ± 0.37	$2.64 \times 10^{-21} \pm 1.48\%$	t_2	1.1×10^6
9	36.53 ± 0.09	$1.51 \times 10^{-21} \pm 0.49\%$	t_1	6.2×10^5
10	36.67 ± 0.17	$9.50 \times 10^{-21} \pm 0.70\%$	t_1	3.9×10^6
14	37.57 ± 0.10	$1.98 \times 10^{-20} \pm 1.28\%$	t_2	8.1×10^6
15	37.74 ± 0.08	$2.53 \times 10^{-20} \pm 1.09\%$	t_2	1.0×10^7
16	38.12 ± 0.30	$1.28 \times 10^{-20} \pm 0.87\%$	t_1	5.6×10^6
17	39.26 ± 0.26	$7.71 \times 10^{-21} \pm 0.57\%$	t_1	3.2×10^6

The dependence of Q_{GB} and $(s\delta D_{GB})_0$ on the tilt angle Θ of the bicrystals is shown in Figs 6(a) and (b), respectively. Consistent with the $s\delta D_{GB}$ results, the Arrhenius parameters decrease at smaller tilt angles with increasing tilt angle. A sharp maximum is adopted at $\Theta = 36.53^\circ$ slightly before the ideal $\Sigma = 5$ CSL GB and in the immediate vicinity of the $\Sigma = 5$ GB the Arrhenius parameters decrease drastically (bicrystal No. 10, $\Theta = 36.67^\circ$). Behind the high coincidence GB, Q_{GB} and $(s\delta D_{GB})_0$ increase with increasing tilt angle Θ. In our opinion this particular behaviour of Q_{GB} and $(s\delta D_{GB})_0$ reflects information of general validity on GB diffusion in bicrystals but also some special features, which depend on the particular properties of the presently investigated set of bicrystals, as will be discussed below.

4. DISCUSSION

4.1. Estimation of the structure dependence of Au GB segregation in Cu bicrystals

Since the Au GB diffusion in Cu bicrystals was studied in the type-B kinetic regime, the orientation dependence of Au GB segregation on the measured GB diffusion parameters $s\delta D_{GB}$ and the determined Arrhenius parameters $(s\delta D_{GB})_0$ and $Q_{GB} =$

Table 7. Results and experimental parameters of ^{64}Cu diffusion along [001] tilt GBs with different tilt angles Θ in symmetrical near $\Sigma = 5$, $\Theta = 36.9^\circ$ (310)[001] GBs. $T = 919$ K, $t = 34\,560$ s, $D = 6.49 \times 10^{-17}$ m^2/s, $\alpha_1 = 1.67 \times 10^{-4}$

No.	Θ (°)	$s\delta D_{GB}$ (m^3/s)	β
6	36.00 ± 0.29	$6.61 \times 10^{-20} \pm 2.3\%$	3.4×10^2
7	36.26 ± 0.37	$5.68 \times 10^{-20} \pm 0.83\%$	2.9×10^2
9	36.53 ± 0.09	$5.85 \times 10^{-20} \pm 0.68\%$	3.0×10^2
10	36.67 ± 0.17	$7.01 \times 10^{-20} \pm 0.58\%$	3.6×10^2
14	37.57 ± 0.10	$7.25 \times 10^{-20} \pm 0.70\%$	3.7×10^2

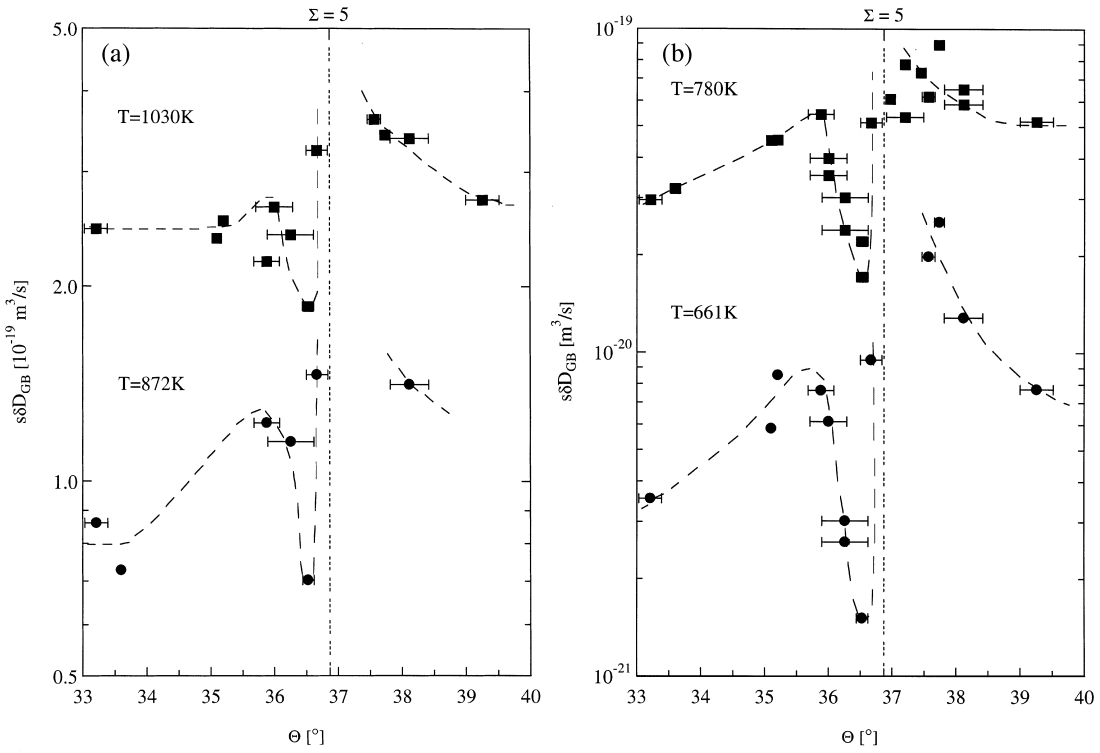

Fig. 3. Dependence of the diffusion parameter $s\delta D_{GB}$ of ^{195}Au diffusion along near $\Sigma = 5$, $\Theta = 36.9°$ (310)[001] Cu tilt GBs on the tilt angle Θ at $T = 1030$ and 872 K (a), $T = 780$ and 661 K (b).

$H_{GB} + H_s$ (H_{GB}: activation enthalpy of GB diffusion, H_s: solute GB segregation enthalpy) have to be considered.

Comparing the orientation dependence of the Au GB diffusion parameters $s\delta D_{GB}$ in Cu, Figs 3(a) and (b), qualitatively with the orientation dependence of GB self-diffusion, Fig. 4, it is evident that the GB diffusion parameter show the same characteristic orientation dependence for GB self- as well as for GB solute diffusion of Au in Cu. This provides convincing evidence that the observed sharp variation of $s\delta D_{GB}$ must be related to the orientation dependence of the GB diffusion coefficient D_{GB}.

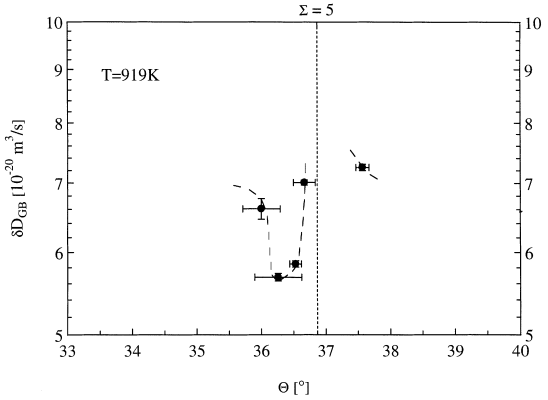

Fig. 4. Dependence of the diffusion parameter δD_{GB} of ^{64}Cu self-diffusion along near $\Sigma = 5$, $\Theta = 36.9°$ (310)[001] Cu tilt GBs on the tilt angle Θ at $T = 919$ K.

Furthermore, the GB segregation of Au in Cu polycrystals was determined in the temperature range 526–450 K by measuring GB diffusion in type-B and type-C kinetic regimes [14]. The temperature dependence of the segregation factor of Au in Cu leads to the Arrhenius parameters $s_0 = 0.88$ and $H_s = -9.7$ kJ/mol on the condition of Henry-type segregation behaviour. Hofmann *et al.* [21] studied the orientation dependence of GB segregation enthalpies of Si, P and C in symmetrical [001] Fe–3.5% Si tilt GBs. The smallest values of H_s are observed at symmetrical GBs of high coincidence. An increasing deviation from the high coincidence orientation reveals increasing values of H_s; maximum values are obtained at general large angle GBs. Taking now into account that the determined H_s value of Au GB segregation in Cu polycrystals can be related to general large angle GBs [14], the variation of H_s with the tilt angle Θ in the vicinity of the ideal $\Sigma = 5$ CSL GB should not exceed 9.7 kJ/mol. As a consequence, the measured variation of $Q_{GB}(\Theta)$ of at least 60 kJ/mol, Fig. 6(a), cannot be explained by segregation effects alone. A considerable part of this variation must be attributed to the structure dependence of GB diffusion.

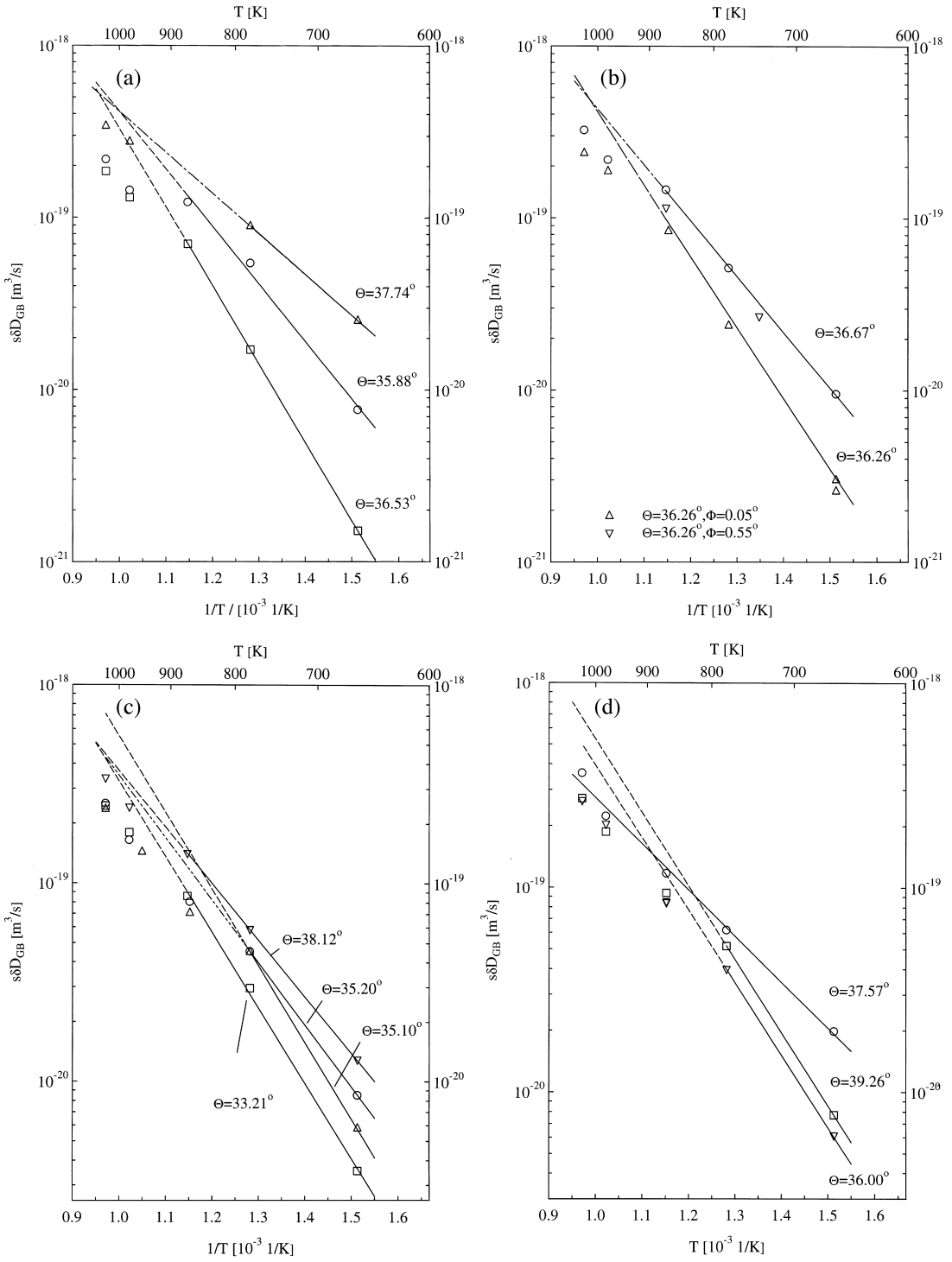

Fig. 5. Temperature dependence of ^{195}Au diffusion along near $\Sigma = 5$, $\Theta = 36.9^\circ$ (310)[001] Cu tilt GBs in Arrhenius coordinates.

4.2. Structure dependence of Au and Cu GB diffusion in Cu bicrystals

The orientation dependence of GB diffusion in the tilt angle range $33.21^\circ \leq \Theta \leq 36.53^\circ$ indicates a cusp of $s\delta D_{GB}$ and maxima of Arrhenius parameters, as determined from the lower temperature data, in the vicinity of the $\Sigma = 5$ CSL GB, see Figs 3 and 6. This behaviour can be well explained in terms of the CSL model. Grain boundaries of high coincidence and therefore of highly ordered atomic structure are expected to yield minima in diffusivity and maxima in Arrhenius parameters due

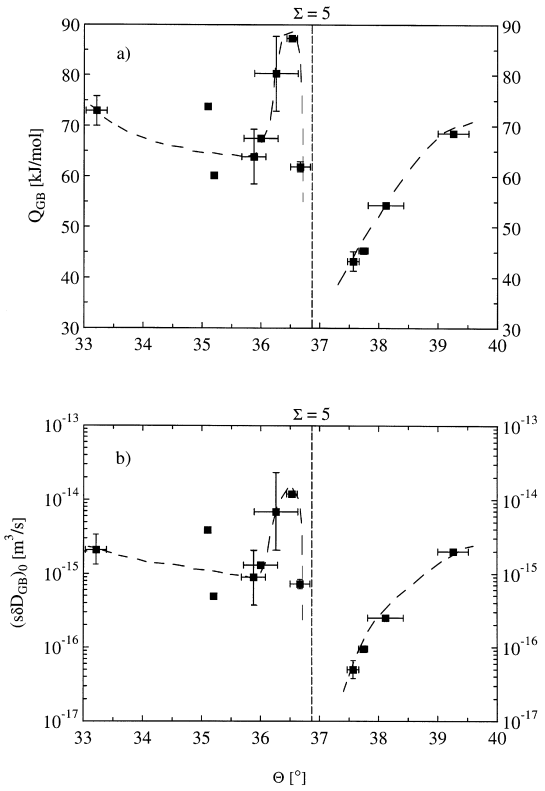

Fig. 6. Dependence of the effective activation enthalpy Q_{GB} (a) and the pre-exponential factor $(s\delta D_{GB})_0$ (b) of ^{195}Au diffusion along near $\Sigma = 5$, $\Theta = 36.9^\circ$ (310)[001] Cu tilt GBs on the tilt angle Θ. The Arrhenius parameters are determined from lower temperature diffusion data.

to the larger mean vacancy formation and migration enthalpies in comparison to GBs of low coincidence and of lower degree of perfection [6]. Small deviations in Θ from the ideal CSL GB are compensated by additionally inserted GB dislocations [22]. Despite small deviations in the tilt angle, the GB core almost keeps the highly ordered atomic structure with the exception, however, of localized additionally inserted GB dislocations. These intrinsic dislocations obviously offer "easy" paths for rapid atomic motion. With increasing tilt deviation $\Delta\Theta$ from the ideal $\Sigma = 5$ GB, the density of the additionally inserted GB dislocations increases and therefore the diffusion flux along the GBs also increases. The CSL model of diffusion was supported by GB diffusion measurements of Ge in oriented Al [111] tilt GBs with orientations near the ideal $\Sigma = 7$, $\Theta = 38.2^\circ$ $(12\bar{3})$[111] CSL GB [17], where a distinct cusp of $s\delta D_{GB}$ was clearly observed at all investigated temperatures and maxima of the Arrhenius parameters were obtained at the ideal $\Sigma = 7$ GB.

Table 8. Arrhenius parameters of ^{195}Au diffusion along Cu GBs with different tilt angles near symmetrical $\Sigma = 5$, $\Theta = 36.9^\circ$ (310)[001] GBs at sufficiently low temperatures. Errors of Q_{GB} are not given if only two points of data were taken into account in the Arrhenius fit

No.	T (K)	$(s\delta D_{GB})_0$ (m^3/s)	Q_{GB} (kJ/mol)
1	661–872	2.1×10^{-15}	72.9 ± 2.9
3	661–780	3.9×10^{-15}	73.8
4	661–780	4.9×10^{-16}	60.2
5	661–872	9.0×10^{-16}	63.9 ± 5.4
6	661–868	1.3×10^{-15}	67.5
7	661–872	6.9×10^{-15}	80.3 ± 7.4
9	661–872	1.2×10^{-14}	87.3 ± 0.1
10	661–872	7.3×10^{-16}	61.9 ± 1.0
14	661–1030	5.0×10^{-17}	43.2 ± 1.9
15	661–780	9.6×10^{-17}	45.3
16	661–872	2.5×10^{-16}	54.3 ± 0.1
17	661–780	2.0×10^{-15}	68.5

In the present study, however, the GB diffusion parameter increases drastically within a few tenths of a degree of Θ in the immediate vicinity of the ideal $\Sigma = 5$ CSL GB, at $\Theta > 36.53^\circ$. This enhancement of $s\delta D_{GB}$ at $\Theta = 36.67^\circ$ of Au is observed at all investigated temperatures, Fig. 3, and also for the GB self-diffusion, Fig. 4. Furthermore, the orientation dependence of the Arrhenius parameters reveals a drastic decrease slightly before the ideal $\Sigma = 5$ CSL GB. It has to be noted that all individual samples of a given orientation were cut from the corresponding same as-grown bicrystal. A critical look at the determined orientation parameters of the used bicrystals, Table 1, reveals that $s\delta D_{GB}$ is enhanced and Q_{GB} and $(s\delta D_{GB})_0$ are small for those bicrystals with comparatively large twist angles Φ. Especially the twist angle Φ of bicrystals No. 10 ($\Theta = 36.67^\circ$, $\Phi = 1.85^\circ$) is the largest one in the presently used set of Cu bicrystals. But also the twist components of bicrystals Nos. 11 and 13–15, just behind the ideal CSL GB, are comparatively large. On the other hand, no significant influence on the GB diffusion is observed from small deviations in the second tilt angle Ψ of the bicrystals, Table 1. The dependence of $s\delta D_{GB}$ on the orientation angle Θ appears rather asymmetric with respect to the ideal $\Sigma = 5$, $\Theta = 36.9^\circ$ orientation. In our opinion this fact results from the presently available set of bicrystals, which accidentally reveal somewhat larger twist angle contributions just for the orientations $36.67^\circ < \Theta < 38.12^\circ$.

The features measured in the course of $s\delta D_{GB}$ and Q_{GB} can be tentatively explained by additionally inserted dislocation structures into the GBs due to the twist and second tilt components of the bicrystals. Vystavel *et al.* [23] studied the dislocation structures of Cu tilt GBs with small deviations in Θ, Φ and Ψ from the ideal $\Sigma = 5$, $\Theta = 36.9^\circ$ (310)[001] tilt GB applying transmission electron microscopy. The investigated Cu bicrystals stem from the same origin as the Cu bicrystals of this study. Figure 7 shows schematically the observed GB dislocation pattern in the boundary plane of these bicrystals. The dislocation structure consists of an array of parallel edge dislocations l_E and of a hexagonal dislocation net. The spacing between the parallel edge dislocations amount to a few 10 nm. The hexagonal dislocation net is composed of three

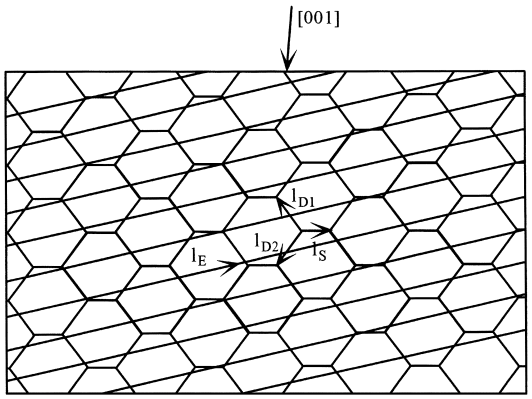

Fig. 7. Schematic illustration of arrays of dislocation lines in the plane of a near $\Sigma = 5$, $\Theta = 36.9^\circ$ (310)[001] Cu tilt GB with small deviations in Θ, Φ and Ψ from the ideal CSL GB [23]. l_E represents the line of edge dislocations forming an array of parallel dislocations; the hexagonal shaped dislocation net consists of the screw dislocation l_S and of l_{D1} and l_{D2} of mixed screw and edge character. The orientation of the [001] axis, which is the diffusional direction, is indicated.

different dislocations: l_S represents dislocations of almost screw character, l_{D1} and l_{D2} are dislocations of mixed screw and edge character. Vystavel *et al.* identified the array of parallel dislocation to be responsible for the second tilt deviation Ψ from the ideal $\Sigma = 5$ CSL GB. The hexagonal dislocation net stems from the twist deviation Φ of the bicrystal from the ideal high coincidence GB. Since the authors determined the directions of the dislocation lines, it is possible to compare them to the diffusion direction of the present GB diffusion experiments, see Fig. 7.

Assuming now that dislocation lines, which are aligned especially parallel to the [001] diffusion direction, contribute to "easy" paths of rapid diffusion, the array of edge dislocations l_E, directed almost perpendicular to the [001] diffusion direction, is expected to be rather ineffective for the GB diffusion. Since these dislocations are formed due to the second tilt deviation Ψ of the GBs, no influence of Ψ on GB diffusion is expected, in agreement with the present results. The dislocation lines l_{D1} and l_{D2} of the hexagonal net are oriented in such a way, that they can represent such paths of rapid diffusion along the [001] direction in the GBs. These paths may be characterized by a comparatively smaller migration enthalpy and/or lower correlation of sequences of atomic jumps [24]. Since the hexagonal dislocation net is formed due to the twist deviation Φ of the bicrystals, the observed influence of the twist angle on GB diffusion can be qualitatively understood.

The observed orientation dependence of Au and Cu GB diffusion is based on two features: on the one hand by a cusp in $s\delta D_{GB}$ and maxima in the Arrhenius parameters exactly at the $\Sigma = 5$ CSL GB due to the highly ordered atomic structure of the CSL GB, on the other hand by additionally inserted "easy" diffusion paths formed due to the twist angle deviations of individual bicrystals, especially in the immediate vicinity of the $\Sigma = 5$ CSL GB. Both features superimpose to the presently observed orientation dependence of GB diffusion which reflects the special "fine structure" of the presently used set of bicrystals. This short discussion clearly demonstrates that results of GB diffusion experiments in real bicrystals can be interpreted in a satisfying manner only, if as much as possible parameters describing the GB structure are accurately known. Furthermore, it is evident that previous diffusion investigations on less well defined bicrystals and GB diffusion profiles require a critical revision.

4.3. Temperature dependence of Au GB diffusion in Cu bicrystals

In Section 3.2 it was already pointed out that in the investigated temperature range the GB diffusion parameter $s\delta D_{GB}$ of Au in Cu does not follow straight lines in the Arrhenius plots, Fig. 5, but reveals a downward curvature at temperatures $T > 800$ K. At sufficiently low temperatures we have approximated the temperature dependence of $s\delta D_{GB}$ by Arrhenius lines and the resulting Arrhenius parameters show a characteristic orientation dependence consistent with the orientation dependence of $s\delta D_{GB}$. At higher temperatures, however, the temperature dependence of $s\delta D_{GB}$ is ambiguous. Due to the lack of a sufficient number of experimental points it is not possible to decide between a straight Arrhenius behaviour or a continuous curvature of $s\delta D_{GB}$.

A continuous curvature in the Arrhenius plot would indicate a decrease of structural order in the GBs with increasing temperature. Molecular dynamic studies [25] support the idea of temperature induced disorder due to an increasing point defect concentration in the GBs. Despite of this, the GB retains the crystalline character even at higher temperatures. That study is not in conflict with the present experimental results. The observed deviations of $s\delta D_{GB}$ at higher temperatures indicate a smaller activation enthalpy of GB diffusion which might be linked to larger defect densities in the GBs. The characteristic orientation dependence of $s\delta D_{GB}$ was observed even at high temperatures [$T = 1030$ K, Fig. 3(a)] which still reveals a crystalline order of the GBs at these temperatures.

On the other hand, the experimental points may be approximated by straight but different Arrhenius lines at high temperatures as well as at low temperatures, respectively. Such an approximation also leads to smaller activation enthalpies of GB diffusion at high temperatures in comparison to the low temperature range, however, a sharp bend or a jump in the diffusivity is expected at a certain temperature. This interpretation supports the idea of a phase transition-like change of the GB structure.

Several investigations on thermodynamic and kinetic properties of GBs indicate a "special to general" GB phase transition at a certain temperature T_c and only below T_c the GBs exhibit special properties [6, 26, 27]. The temperature T_c itself depends on the magnitude of the deviation in orientation from the special high coincidence GB. With increasing deviation from the ideal CSL GB T_c is expected to decrease.

Furthermore, recent molecular dynamics simulations of self-diffusion in GBs in f.c.c. metals indicate a transition from "solid-like" to "liquid-like" diffusion at elevated temperatures [28]. At high temperatures the GB diffusion is characterized by the same universal atomic mobility and by a low activation enthalpy, in comparison to lower temperatures, where the GB diffusion is "solid-like" [28]. The temperature, where this transition occurs, depends on the GB energy of the CSL GB. In CSL GBs with fairly large GB energies, such as the presently studied $\Sigma = 5$ CSL GB, the transition "solid-like" to "liquid-like" diffusion is predicted at roughly $0.65T_m$ (T_m: melting temperature). In GBs with comparatively lower energies, e.g. $\Sigma = 7$, $\Theta = 38.2^\circ$ $(12\bar{3})[111]$ CSL GB, the crystalline-like diffusion is expected to occur up to $\approx 0.9T_m$ [28]. This prediction is in agreement with our recent diffusion results of Ge in near $\Sigma = 7$ [111] tilt GBs of Al [17] where indeed no curvature in the Arrhenius dependencies was observed in the investigated temperature range 0.56–$0.73T_m$.

On the basis of the present experimental results it is difficult to give a consistent explanation of the observed non-Arrhenius behaviour of $s\delta D_{GB}$ data.

5. SUMMARY AND CONCLUSIONS

- The parameter $s\delta D_{GB}$ of ^{195}Au diffusion and δD_{GB} of ^{64}Cu diffusion along symmetrical $\Sigma = 5$, $\Theta = 36.9^\circ$ (310)[001] Cu GBs strongly depends on the tilt angle Θ. The GB diffusion of solute and of solvent atoms show characteristic cusps not exactly at but slightly below the ideal $\Sigma = 5$ CSL GB. In the immediate vicinity of the $\Sigma = 5$ CSL GB the GB diffusion parameter increases. This behaviour is reproducibly observed for all investigated temperatures.
- The temperature dependence of $s\delta D_{GB}$ of Au GB diffusion was approximated by Arrhenius relations at lower temperatures. The resulting Arrhenius parameters show the opposite behaviour in comparison to $s\delta D_{GB}(\Theta)$. A characteristic peak in Q_{GB} and $(s\delta D_{GB})_0$ is observed slightly below the tilt orientation of the ideal $\Sigma = 5$ CSL GB. At higher temperatures, however, a downward curved deviation from the linear Arrhenius relation is observed for almost all investigated GBs.
- The particular orientation behaviour of GB diffusion in the present study can be explained by the superposition of two features: on the one hand, GB diffusion is generally influenced by the highly ordered atomic structure of the $\Sigma = 5$ high coincidence CSL GB, where cusps in $s\delta D_{GB}$ and peaks in the Arrhenius parameters exactly at the ideal $\Sigma = 5$ GB are expected. On the other hand, the additionally inserted net of GB dislocations formed due to the small twist deviations Φ from the ideal $\Sigma = 5$ GB in our real bicrystals provides additional paths of "easy" diffusion. Especially, the GBs in the immediate vicinity of the $\Sigma = 5$ GB reveal (as an accidental result of the production process) relatively large twist angles. Therefore, the cusps in $s\delta D_{GB}(\Theta)$ and peaks in the Arrhenius parameters expected at $\Theta = 36.9^\circ$ are masked to some extent and are only apparently shifted to a lower value in Θ.
- The deviation of $s\delta D_{GB}(T)$ from the straight Arrhenius dependence at higher temperature indicates a temperature induced change of the GB structure. Within the scope of the limited number of experimental results, it is not possible to decide whether a continuous curvature, a sharp bend or a jump occurs at a certain temperature. Therefore, the nature of the temperature induced change of the GB structure requires further detailed considerations.

Acknowledgements—This work was supported by the German Ministry of Research and Technology (BMBF) under contract No. 03HE3MUE. The authors would like to thank S. S. Khasanov for the determination of the orientations of the bicrystals. One of the authors (S. Prokofjev) thanks the Russian Foundation for Fundamental Researches for support (contract No. 96-02-48840). The production of the ^{64}Cu isotope was performed with support of the reactor service group of the Research Center Geesthacht, Germany.

REFERENCES

1. Aleshin, A. N., Bokshtein, B. S. and Shvindlerman, L. S., *Soviet Phys. Solid St.*, 1977, **19**, 2051.
2. Aleshin, A. N., Aristov, V. Y., Bokshtein, B. S. and Shvindlerman, L. S., *Physica status solidi (a)*, 1978, **359**, 1256.
3. Aleshin, A. N., Prokofjev, S. I. and Shvindlerman, L. S., *Scripta metall.*, 1985, **19**, 1135.
4. Aleshin, A. N., Prokofjev, S. I. and Shvindlerman, L. S., *Defect Diffusion Forum*, 1989, **66–69**, 861.
5. Li, X. M. and Chou, Y. T., *Acta mater.*, 1996, **44**, 3535.
6. Straumal, B. B., Klinger, L. M. and Shvindlerman, L. S., *Acta metall.*, 1984, **32**, 1355.
7. Ma, Q. and Balluffi, R. W., *Mater. Res. Soc. Symp.*, 1991, **209**, 33.
8. Sommer, J., Herzig, Chr., Mayer, S. and Gust, W., *Defect Diffusion Forum*, 1989, **66–69**, 843.
9. Ma, Q. and Balluffi, R. W., *Acta metall. mater.*, 1993, **41**, 133.
10. Balluffi, R. W. and Brokman, A., *Scripta metall.*, 1983, **17**, 1027.

11. Balluffi, R. W., in *Diffusion in Crystalline Solids*, ed. G. E. Murch and A. S. Nowick. Academic Press, New York, 1984.
12. Massalski, T. B. (ed.), *Binary Alloy Phase Diagrams*. Am. Soc. Metals, Metals Park, Ohio, 1986.
13. Kaur, I., Mishin, Y. and Gust, W., *Fundamentals of Grain and Interphase Boundary Diffusion*. Wiley, Chichester, 1995.
14. Surholt, T., Mishin, Y. M. and Herzig, Chr., *Phys. Rev. B*, 1994, **50**, 3577.
15. Fujikawa, S., Werner, M., Mehrer, H. and Seeger, A., *Mater. Sci. Forum*, 1987, **15–18**, 431.
16. Maier, K., *Physica status solidi (a)*, 1977, **44**, 567.
17. Surholt, T., Molodov, D. A. and Herzig, Chr., *Acta mater.*, 1998, **46**, 5345.
18. Surholt, T., Minkwitz, C. and Herzig, Chr., *Acta mater.*, 1998, **46**, 1849.
19. Güthoff, F., Mishin, Y. and Herzig, Chr., *Z. Metallk.*, 1993, **84**, 584.
20. Köppers, M., Mishin, Y. and Herzig, Chr., *Acta metall. mater.*, 1994, **42**, 2859.
21. Hofmann, S., Lejceck, P. and Adamek, J., *Surf. Interface Anal.*, 1992, **19**, 601.
22. Schober, T. and Balluffi, R. W., *Phil. Mag.*, 1970, **21**, 109.
23. Vystavel, T., Paidar, V., Gemperle, A. and Gemperlova, J., *Interface Sci.*, 1997, **5**, 215.
24. Mishin, Y., *Phil. Mag. A*, 1995, **72**, 1589.
25. Ciccoti, G., Guillope, M. and Pontikis, V., *Phys. Rev. B*, 1983, **27**, 5576.
26. Maksimova, E. L., Shvindlerman, L. S. and Straumal, B. B., *Acta metall.*, 1988, **36**, 1573.
27. Maksimova, E. L., Rabkin, E. I., Shvindlerman, L. S. and Straumal, B. B., *Acta metall.*, 1989, **37**, 1995.
28. Keblinski, P., Phillpot, S. R., Wolf, D. and Gleiter, H., *Phys. Rev. Lett.*, 1996, **77**, 2965 and Private communication.